Article

Tribological Properties of Ti6Al4V Titanium Textured Surfaces Created by Laser: Effect of Dimple Density

Akshay Gaikwad [1], Juan Manuel Vázquez-Martínez [2], Jorge Salguero [2] and Patricia Iglesias [1,*]

1 Mechanical Engineering Department, Rochester Institute of Technology, 72 Lomb Memorial Drive, Rochester, NY 14623, USA; agg7834@rit.edu
2 Department of Mechanical Engineering and Industrial Design, School of Engineering, University of Cadiz, Av. Universidad De Cádiz 10, E-11519 Puerto Real, Spain; juanmanuel.vazquez@uca.es (J.M.V.-M.); jorge.salguero@uca.es (J.S.)
* Correspondence: pxieme@rit.edu; Tel.: +1-585-475-7694

Abstract: The loss of energy due to friction is one of the major problems industries are facing nowadays. Friction and wear between sliding components reduce the mechanical efficiency of machines and have a negative impact on the environment. In recent years, surface texturing has shown tremendous ability to reduce friction and wear. Micro-features generated on surfaces act as a secondary reservoir for lubricants and wear debris receptacles to further reduce abrasion. In addition, surface texturing boosts hydrodynamic pressure, which increases the elasto-hydrodynamic lubrication regime of the Stribeck curve, reducing friction and wear. Amongst all different techniques to texture surfaces, laser texturing is the most popular due to its advantages such as high accuracy, good consistency and celerity as compared to other techniques. This study investigated the effect of laser texturing on the tribological properties of Ti6Al4V in contact with a ceramic ball. The effect of varying the dimple density on friction and wear was studied using a ball-on-flat reciprocating tribometer under lubricated conditions. Results show that friction and wear were reduced for all the textured samples as compared to an untextured sample, with important friction and wear reductions for the samples with the highest dimple densities. For samples with intermediate dimple densities, the friction coefficient stayed low until the dimples wore out from the surface and then increased to a value similar to the friction coefficient of the untextured surface. The dimple wear-out time observed in these specimens was greatly influenced by the dimple density.

Keywords: textured surfaces; friction; wear; lubrication; titanium

1. Introduction

The good mechanical strength, low density, excellent corrosion resistance and biocompatibility of titanium alloys make them ideal candidates for aerospace [1,2], automotive [3,4] and biomedical applications [5,6]. Nevertheless, the poor tribological properties of these alloys are a major drawback to their application.

Friction between mechanical components is responsible for important energy losses and has a negative environmental impact [7–11]. Furthermore, wear is behind a large proportion of mechanical failures [12]. Globally, energy consumed due to friction and wear in industries is around 103 EJ and 16 EJ, respectively [2,3]. In the transportation industry, for example, friction consumes almost 60% of the energy produced [7]. The cost incorporated to overcome this friction and replace/remanufacture worn parts in industries is estimated to be USD 285.5 billion [7]. In addition to these economic losses, friction and wear indirectly cause global emissions of around 7040 $MtCO_2$ and 1080 $MtCO_2$, respectively, every year [7].

There are different techniques that can be used to reduce friction and wear between two relatively moving surfaces, such as the use of high-performance lubricants [13,14], advanced materials [15], surface modifications [16], and other modern technologies. Among all of these techniques, surface texturing has attracted the attention of the tribology community as

an environmentally friendly [17–19] and biocompatible [20] method to improve the friction and wear resistance of a material [21]. Texturing has a positive impact on the loading capacity of materials and friction coefficients [22]. In texturing, artificial micro-features (dimples) are created on the surface, where the wear debris may be trapped, reducing and/or eliminating the plowing effect of friction. Sometimes, these dimples can also act as a reservoir for lubricant. Due to these positive effects, the use of textured surfaces may reduce the coefficient of friction by 75% for starved lubrication [23–25]. Nowadays, the use of textured surfaces is common in mechanical applications such as piston rings, thrust bearings, and face seals [26,27]. Surface texturing can help reduce the energy consumption and emission of CO_2 gases. Textured surfaces improve the wettability and lubrication properties of metals [28,29]. As a result, in vehicles, power output, emissions, and fuel consumption can be considerably improved [30]. Texturing the surface also shows positive variation in the *Stribeck* curve. The textured surfaces produced by modulation-assisted machining accelerate the appearance of the elasto-hydrodynamic regime with friction reduction of 56% and wear reduction of 90% [25,31]. Depending on the design parameters, the effectiveness of surface texturing varies. Design parameters can be size, shape, and density or features such as speed and load [32–35]. Several studies have showed that dimple shape and depth are essential parameters to enhance the friction and wear properties of surfaces [36,37]. While some studies have indicated that dimple density also has a significant effect on the tribological properties of surfaces, no consensus has been reached on an optimum dimple density [36,38], and further research is needed, particularly for titanium alloy surfaces.

There are different methods that could be used to texture metallic surfaces. These methods include sandblasting, acid etching, media blasting, modulation-assisted machining, electron-beam, ion-beam laser texturing [39–41]. Each of the above techniques has its own advantages and disadvantages, but laser texturing is the most popular due to advantages such as high accuracy, good consistency [27,42] and celerity as compared to other techniques. In addition, since there is no waste generated in laser texturing, it can be considered an environmentally friendly method.

In this work, the friction and wear behavior of titanium-textured samples generated by laser were studied under lubricated conditions against a ceramic ball using a ball-on-flat reciprocating tribometer. The effect of varying dimple density on the hardness, contact angle, roughness and tribological properties was also examined.

2. Materials and Methods

2.1. Samples

Ti6Al4V titanium samples were textured using a Rofin EasyMark F20 laser marking machine (ROFIN-SINAR Technologies Inc., Plymouth, MI, USA). Eight different laser velocities were used to texture the surface of a titanium plate (50 mm × 48 mm × 5 mm), obtaining eight different samples with varying dimple densities. Sample 9 represents the untextured sample.

The composition of the Ti6Al4V alloy used in this study is listed in Table 1.

Table 1. Nominal chemical composition of Ti6AlV4 (wt.%).

| Element	%
Ti	balanced
Al	6%
V	4%
Fe	<0.25%
O	<0.2%

Table 2 summarizes the laser texturing conditions for each sample and the resulting dimple density and depth. Sample 1 was created with the lowest laser scanning speed of 400 mm/s and the shorter spacing between two laser paths (20 μm), resulting in the highest

dimple density (50 dimples/mm). Sample 2 through sample 8 were created by using laser speeds ranging from 800 mm/s to 2800 mm/s, respectively, yielding dimple densities that ranged from 25 dimples/mm to 7.1 dimples/mm. Dimple depth varied between 6–8 μm.

Table 2. Laser parameters and resulting dimple density and depth.

| Sample No.	Laser Spot Size (μm)	Laser Speed (mm/s)	Laser Frequency (Hz)	Spacing between Two Laser Passes (μm)	Dimple Density (dimples/mm)	Dimple Depth (μm)
Sample 1	60	400	20,000	20	50	6
Sample 2	60	800	20,000	40	25	6
Sample 3	60	1200	20,000	60	16.7	8
Sample 4	60	1600	20,000	80	12.5	7
Sample 5	60	2000	20,000	100	10	7
Sample 6	60	2400	20,000	120	8.3	7
Sample 7	60	2600	20,000	140	7.6	8
Sample 8	60	2800	20,000	160	7.1	7
Sample 9	Untextured	-	-	-	-	-

Figure 1a shows the schematic representation of variation in dimple density and Figure 1b shows the actual metal samples used for the tests. In addition, the optical microscopic images of the samples are shown in Figure 2. In this work, a nanosecond laser was used for the irradiation of the textures, which implied that some thermal effects modified the size and geometry of the dimples. This effect was mainly related to the energy density of pulses and the scanning speed of the beam used in the irradiation treatments. The variability between the theoretical (Figure 1a) and real geometries (Figure 2) of the textures was due to the accumulation of solidified material at dimple boundaries and material removal.

(**a**)　　　　　　　　　　　　　　　　　　　　　　(**b**)
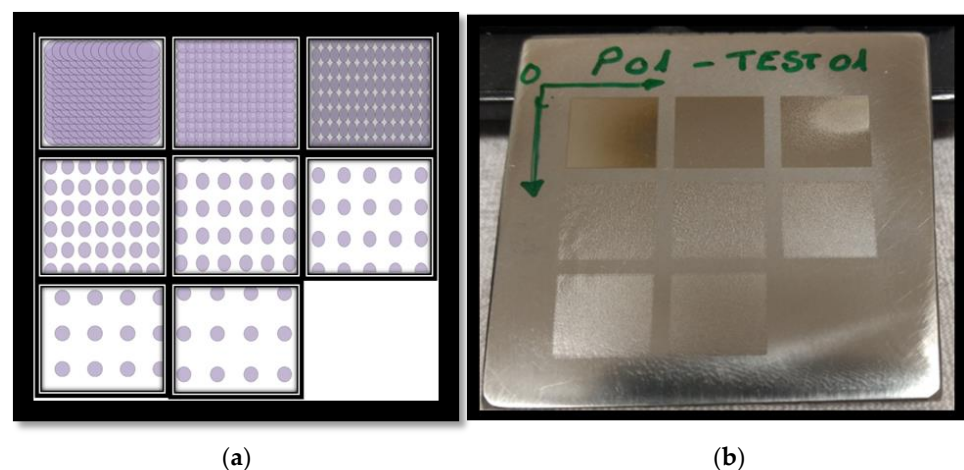
Figure 1. (**a**) Schematic representation of variation in dimple density. (**b**) Variation in dimple density on the actual sample.

2.2. Contact Angle Tests

Contact angle tests were performed on each sample using a Rame-Hart goniometer (Ramé-hart Instrument Co., Succasunna, NJ, USA) and Drop-Image software (Ramé-hart Instrument Co., Succasunna, NJ, USA) to study the wetting effect of the treatments. Polyal-phaolefin (PAO) was used as a liquid over the Ti6Al4V textured surface. These tests were conducted using 2 microliters of PAO for around 24 s to collect 25 data points on contact angles for each sample of Ti6Al4V.
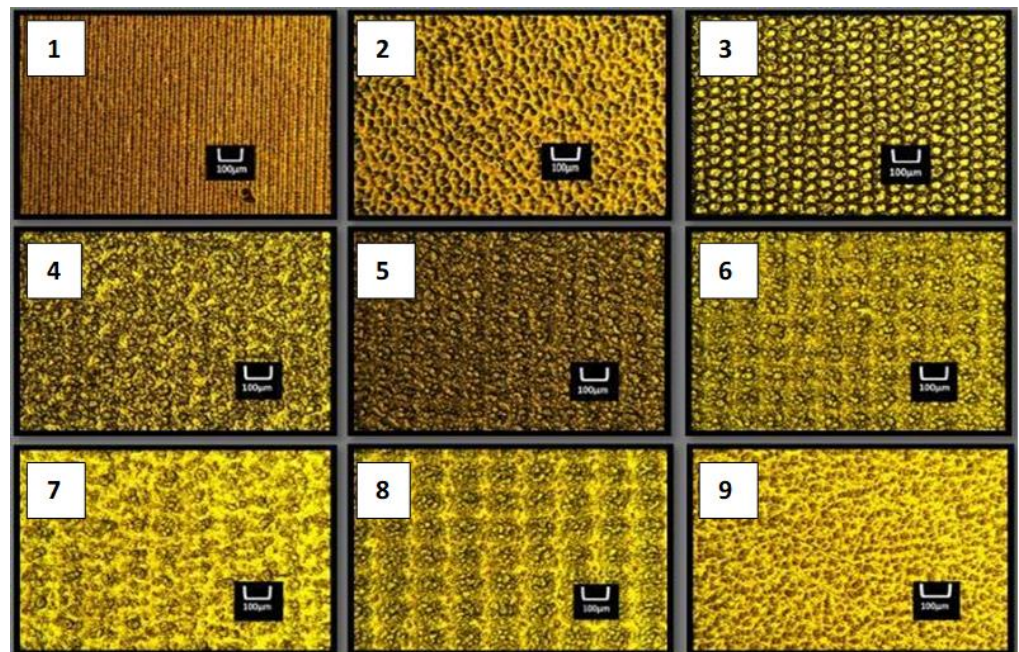
Figure 2. Microscopic images of the samples.

2.3. The Roughness of Textured Surfaces

Roughness tests were performed on all of the samples to find the Ra, Rz, and Rpk values using the NANOVEA ST400 non-contact profilometer (Nanovea Inc., Irvine, CA, USA) with lateral resolution of 1.7 micrometers and vertical resolution of 8 nanometers. Ra is the arithmetic average of the absolute values of the roughness profile ordinates, Rz is the arithmetic mean value of the single roughness depths of consecutive sampling lengths, and Rpk is a functional roughness parameter based on bearing curves commonly used for tribological applications. According to ISO 13565, the Rpk roughness parameter describes the average height of the protruding peaks above the roughness core profile. It represents the portion of the asperities that will be worn away in the first cycle of the dynamic contact of the sliding test.

2.4. Surface Hardness Test

Though laser texturing has several advantages over different texturing processes, it generates heat while the texturing process is underway. Because of the generated heat, the surface of the metal sample may receive an undesirable heat treatment, which could increase the sample surface hardness. This increase in surface hardness may impact the tribological properties of the material. To investigate only the effect of surface hardening due to laser texturing, surface hardness tests were performed using a Vickers micro hardness tester (Mitutoyo MVK-H1, Mitutoyo America Corporation, Aurora, IL, USA). For each sample, 25 readings were recorded at different locations inside the sample.

2.5. Tribological Tests

Tribological tests were performed to calculate the friction coefficient and wear on the titanium textured surfaces against 1.5 mm diameter tungsten carbide balls. A custom-made reciprocating ball-on-flat tribometer (Figure 3a) was used to conduct the tests using PAO as a lubricant. Each test was performed under the same operating conditions, with a normal load of 5 N, which corresponds to a maximum contact pressure of 3.8 GPa. The frequency used was 2 Hz with a stroke length of 3 mm and a total sliding distance of 50 m. After performing the friction tests, wear tracks were analyzed using an OLYMPUS B-2 optical microscope (Olympus, Tokyo, Japan). Volume losses were determined from the mean value

of the wear track width, based on at least 20 measurements made along the wear track (Figure 3b) and using Equation (1) [43]:

$$V_f = L_s[R_f{}^2 \arcsin(\frac{W}{2R_f}) - \frac{W}{2}(R_f - h_f)] + \frac{\pi}{3}h_f{}^2(3R_f - h_f) \qquad (1)$$

where V_f is wear volume in mm^3, L_s is stroke length in mm, W is wear track width in mm, R_f is the radius of the ball in mm, and h_f is wear depth in mm, which is calculated from Equation (2).

$$h_f = R_f - \sqrt{R_f^2 - \frac{W^2}{4}} \qquad (2)$$
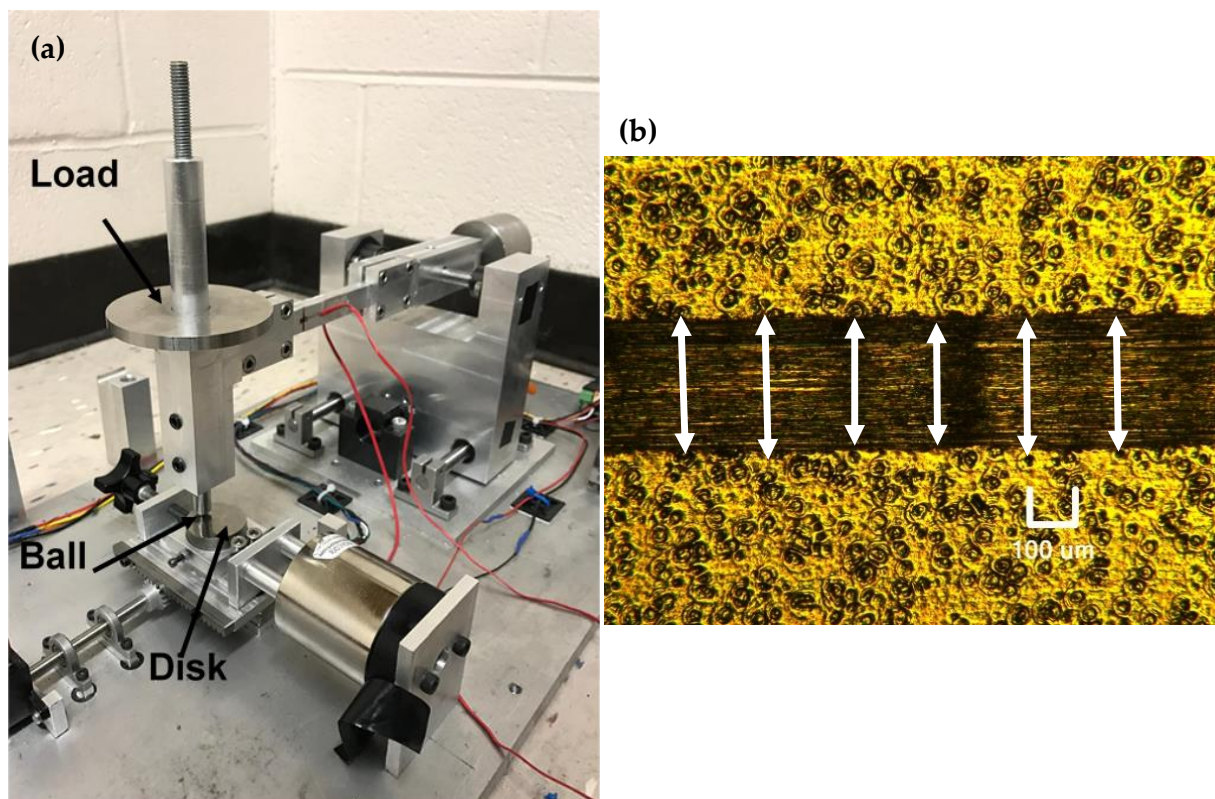
Figure 3. (**a**) Custom-made reciprocating tribometer and (**b**) wear track measurements.

For each sample, at least 3 tests were performed to guarantee the repeatability of the results.

3. Results

3.1. Wettability

The affinity of a surface for a lubricant, also known as wettability, can be characterized by the contact angle [44,45]. In general, low contact angles means good affinity (good wettability) between the liquid and the surface [46,47] (Figure 4). The graph in Figure 5 shows the average (and standard deviation) contact angle of PAO on the titanium textured and untextured surfaces. The contact angle for the untreated sample was higher compared to that of the textured surfaces. Lower contact angles mean higher wettability (better retention of lubricant) of the liquid towards the textured surfaces, which is favorable for friction reduction [47].
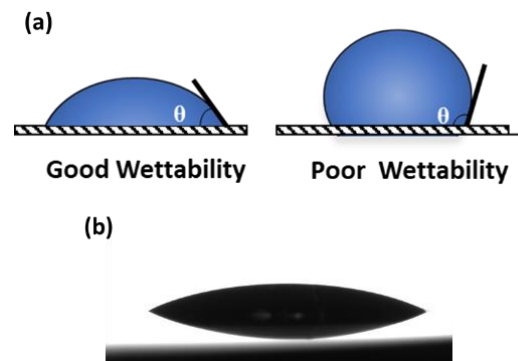
Figure 4. (**a**) Schematic of contact angle showing good and poor wettability and (**b**) picture of contact angle of one PAO drop on a textured surface.
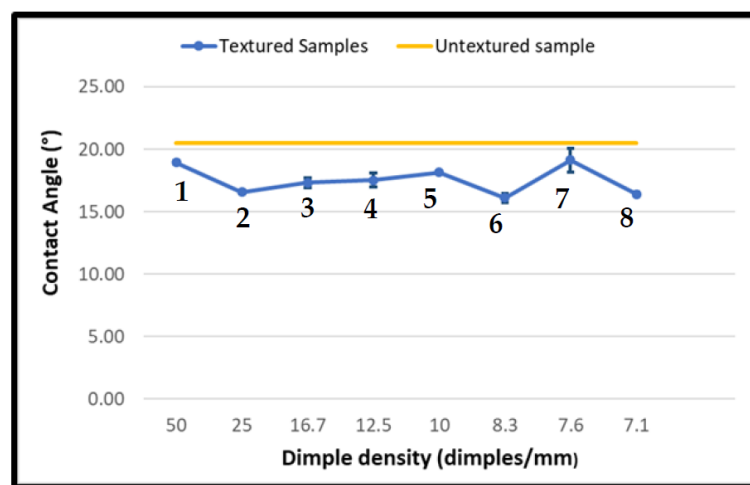

Figure 5. Average contact angles of PAO on textured surfaces. The yellow straight line represents the value of the contact angle on the untextured surface.

3.2. Surface Roughness

Figure 6 shows the Ra, Rz and Rpk roughness values for untextured and textured samples. The yellow line in the figure represents the values for the untextured surface.
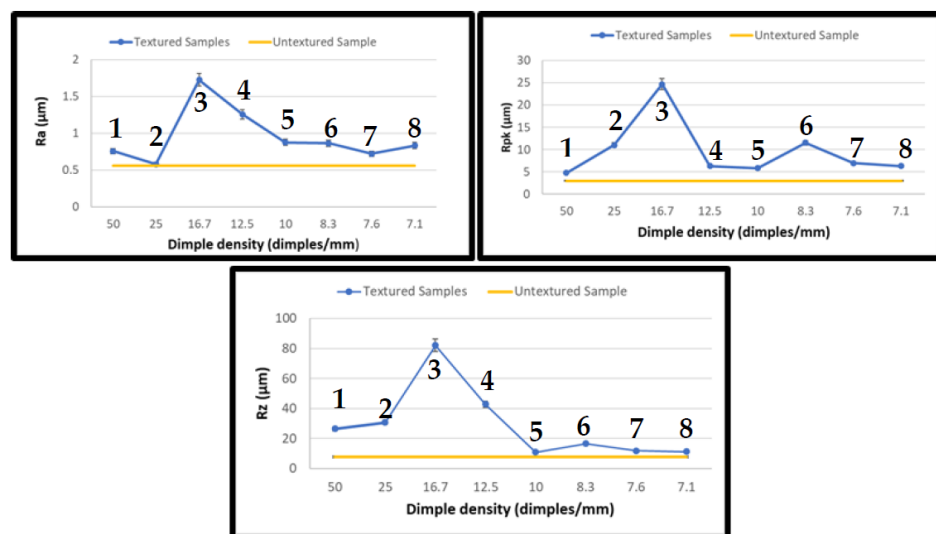

Figure 6. Ra, Rz and Rpk average (and standard deviation) roughness values for untextured (points) and textured (straight line) samples.

As expected, the three measured roughness parameters of the untreated surface were lower than those of the textured surfaces. The sample produced with a laser speed of 1200 mm/s (sample 3), showed the highest values for the three roughness parameters compared to all textured surfaces. In this sample, the borders of the dimples were overlapping each other, resulting in higher roughness values.

3.3. Surface Hardness

Figure 7 compares the average (standard deviation also represented) Vickers hardness values of the textured samples to the hardness value of the untextured sample. From the figure, sample 1, created with a lower laser speed of 400 mm/s and the highest dimple density, showed the highest surface hardness probably due to longer exposure to the laser heat as compared to the other samples. Samples created with laser velocities ranging from 1200 mm/s to 2800 mm/s (samples 3 to 8) showed surface hardness similar to that of the untextured surface, and sample 2 (laser velocity of 800 mm/s), showed a very slight increase in surface hardness.
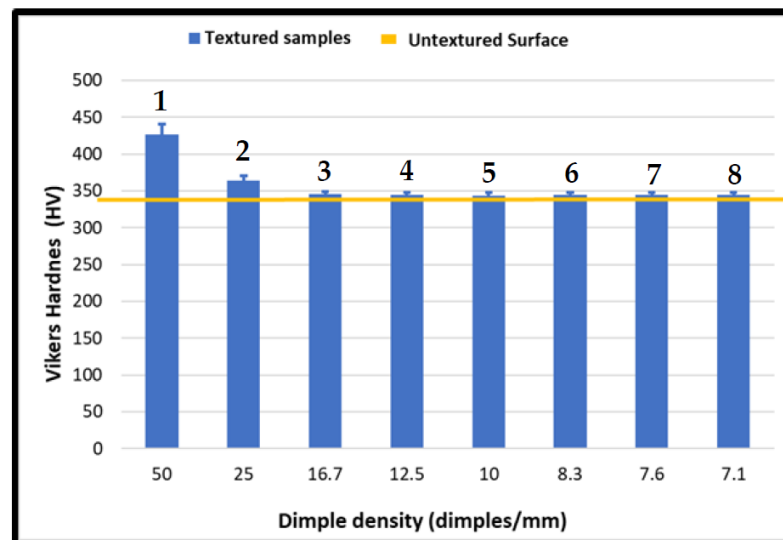

**Figure 7.** Vickers hardness results for textured (bars) and untextured (line) samples.

3.4. Tribological Results

Figure 8 shows the average friction coefficient values obtained from the ball-on-flat reciprocating tribometer tests, when the samples were tested against ceramic balls. The yellow straight line represents the friction coefficient for the untextured sample. Friction coefficients for all textured surfaces were reduced compared to that of the untextured sample, but this reduction was particularly important (~67%) for samples 1 and 2 (samples with the highest dimple density). It is important to note that sample 1, or the sample created with a laser speed of 400 mm/s and dimple density of 50 dimples/mm, showed an important increase in its hardness values that may affect its tribological properties. In sample 2, however, the hardness value remained constant after the surface texturing treatment, by which the friction reduction observed was mainly due to the texturing effect. It is well known that some textures on bearing surfaces may act as lubricant reservoirs and boost hydrodynamic pressure, enhancing surface separation and reducing friction [48–50]. Some textures also may act as receptacles for wear debris, reducing scratching due to a three-body wear effect [16]. Samples with dimple densities ranging from 16.7 to 7.1 dimples/mm (sample 3 to sample 8), all had highly similar friction coefficients, which were slightly lower than that of the untextured sample, showing an average reduction in friction of 6%.
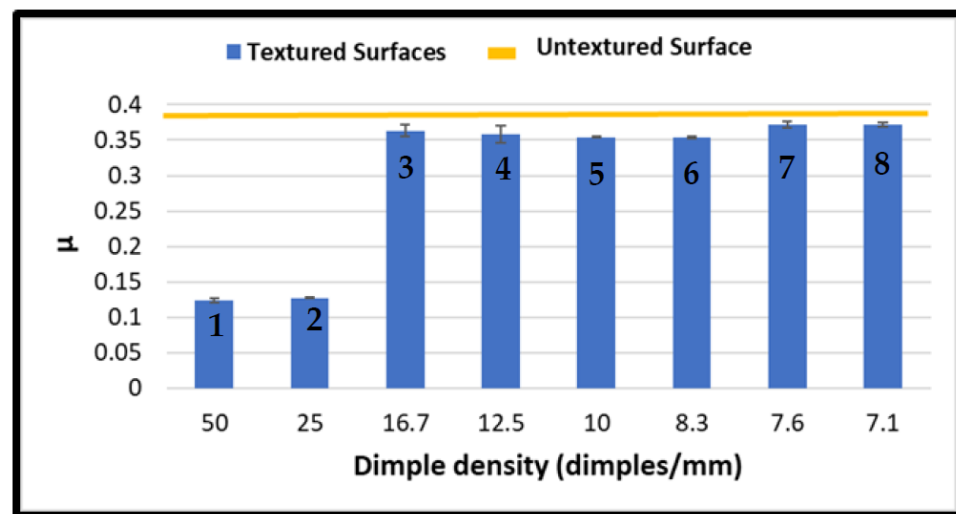
Figure 8. Friction coefficient of textured (bars) and untextured (line) samples against ceramic balls.

The important friction reduction when textured sample 2 was used can be clearly seen in the friction vs. time curves shown in Figure 9. From this figure, we can also see that textured sample 2 did not show the break-in period at the beginning of the tests, which is typically due to the initial removal of asperities. The absence of this high friction period at the beginning of the test has been previously reported [51,52] for other textured surfaces, where the texturing effect maintains low with constant fiction values. It was also very remarkable to see that when the continuous value of friction was represented for the other textured surfaces (Figure 10), all samples started the test with low friction values (no break-in period), and a sudden increment in friction was seen in all of these samples after some time. At the beginning of the test, there were still fresh dimples on the surfaces, and the friction coefficients remained low for a period of time probably due to the better retention of the oil in the textured surfaces [48]. As the test progressed, the textures created in samples 3–8 were not sufficient to retain a lubricant layer between the contacting surfaces, and asperity interactions took place, which eventually wore the dimples out. As a result, the metal surfaces started to perform as untextured surfaces, reaching higher friction values.
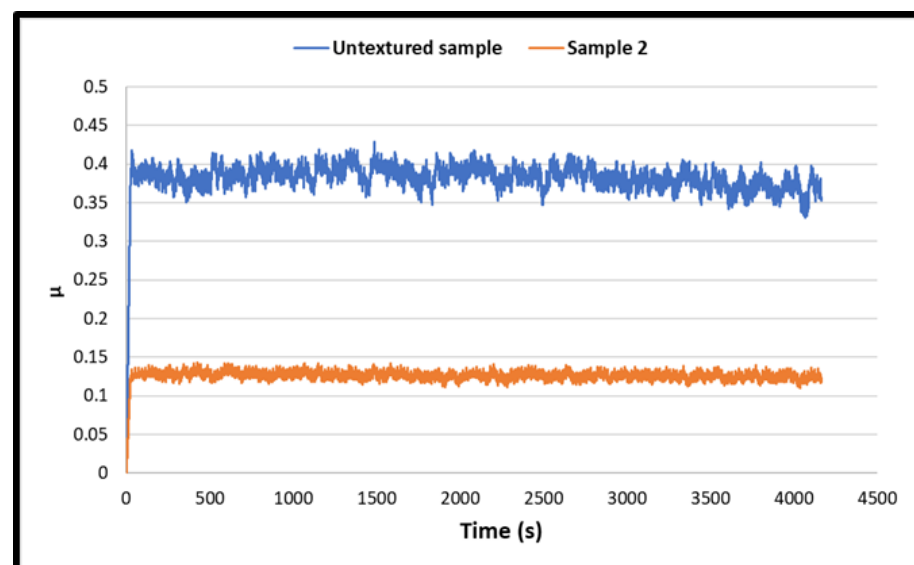

Figure 9. Friction vs. time curves for sample created with laser speed of 800 mm/s and dimple density of 25 dimples/mm (sample 2) and untextured sample.
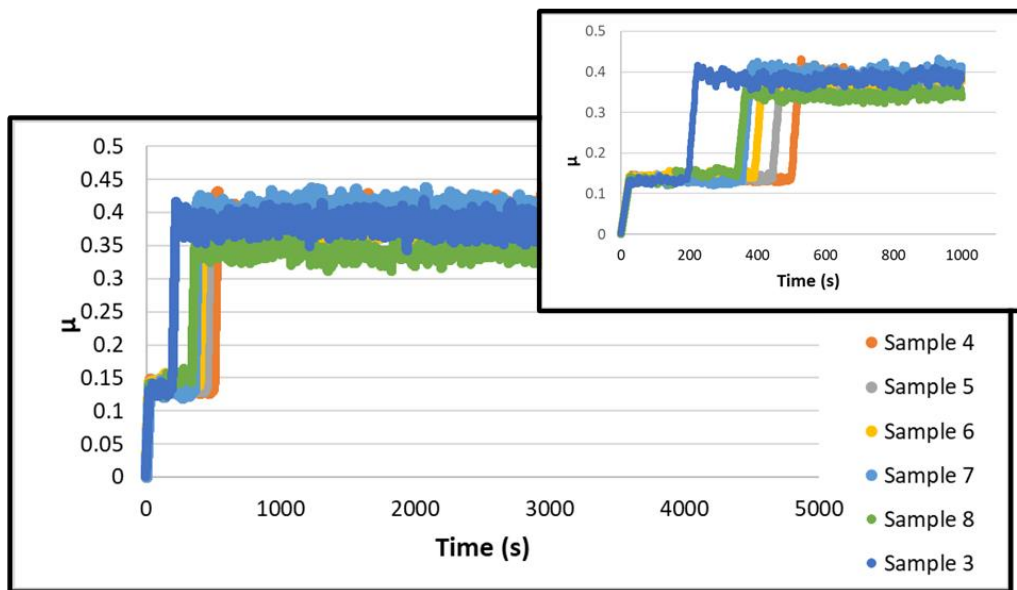
Figure 10. Friction coefficient vs. time curves for samples with dimple densities ranging from 16.7 to 7.1 dimples/mm (sample 3 to sample 8). Detail of friction coefficient vs. time curve for the first 1000 s (sample 3 to sample 8).

If only the first 1000 s (detail inset in Figure 10) are represented in the figure, we can confirm that the period of low friction was different for each sample. The dimple wear-out times for sample 3 to 8 are summarized in Figure 11. From Figures 10 and 11, sample 3 (16.7 dimples/mm) showed the shortest time to wear the dimples out, probably due to the higher surface roughness of this sample amongst all the samples (Figure 6), which promoted the asperity interactions between surfaces. For samples with dimple densities ranging from 12.5 to 7.1 dimple/mm (sample 4 to sample 8), the wear-out time decreased with the decrease in dimple density, with the longest time duration for sample 4 and the shortest duration for sample 8.
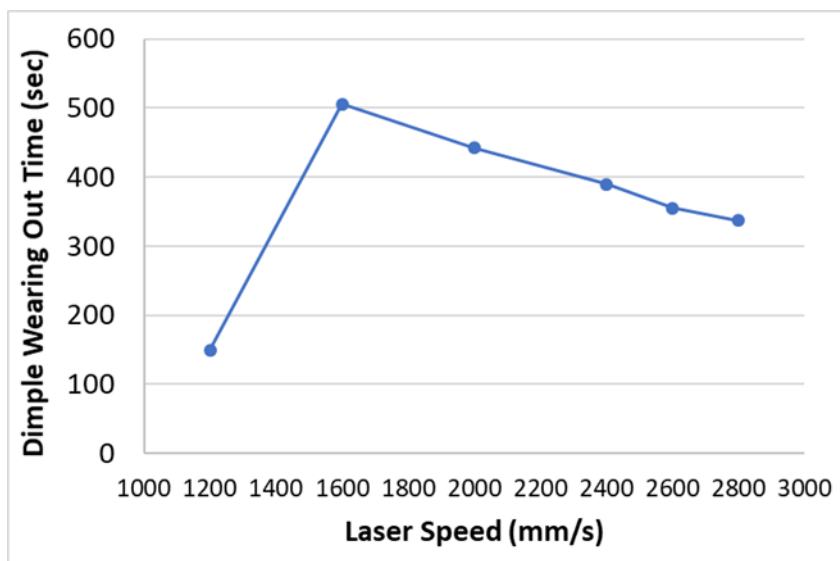
Sample #	Time to wear out dimples (s)
3	150
4	506
5	442
6	390
7	355
8	340

Figure 11. Dimple wear-out time for textured samples with dimple densities ranging from 12.5 to 7.1 dimples/mm (sample 4 to sample 8).

Figure 12 shows the wear volume of the titanium samples after the ball-on-flat reciprocating tests. The solid straight line indicates the wear volume for the untextured sample.

Texturing the surfaces of titanium reduced the wear volume in all samples compared to the untextured surface. Samples 1 (50 dimples/mm) and 2 (25 dimples/mm) showed an impressive wear reduction of almost 99% compared to the untextured sample. Nevertheless, the wear reduction of sample 1, as discussed before, may be due to the heat treatment effect of the laser technology. Sample 2, however, with 25 dimples/mm, showed a very low increase in surface hardness and negligible wear. Samples 3–8 had highly similar wear losses, which were slightly lower than the untextured sample with average wear volume reduction of 11%.
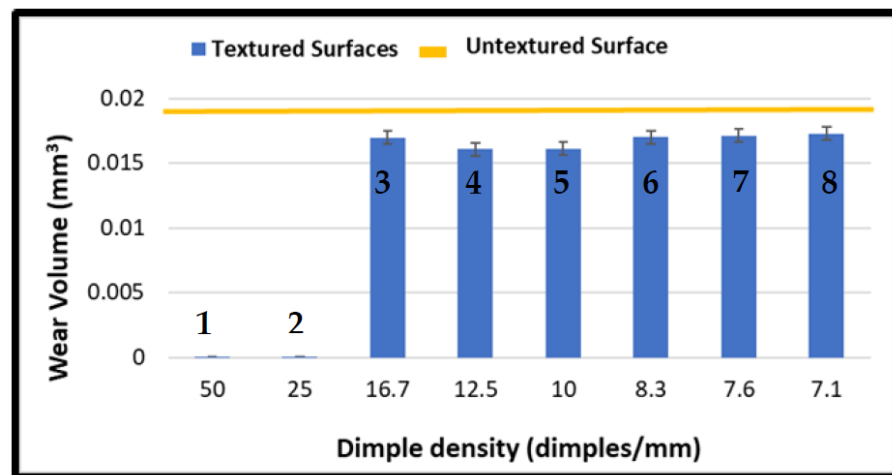

Figure 12. Wear volume on titanium for textured (bars) and untextured (line) samples.

Figure 13 shows the wear track images for the sample with dimple density of 25 dimples/mm (sample 2) and the untextured sample. While the untextured surface showed severe wear with a very wide wear track, the textured surface resulted in almost negligible wear.
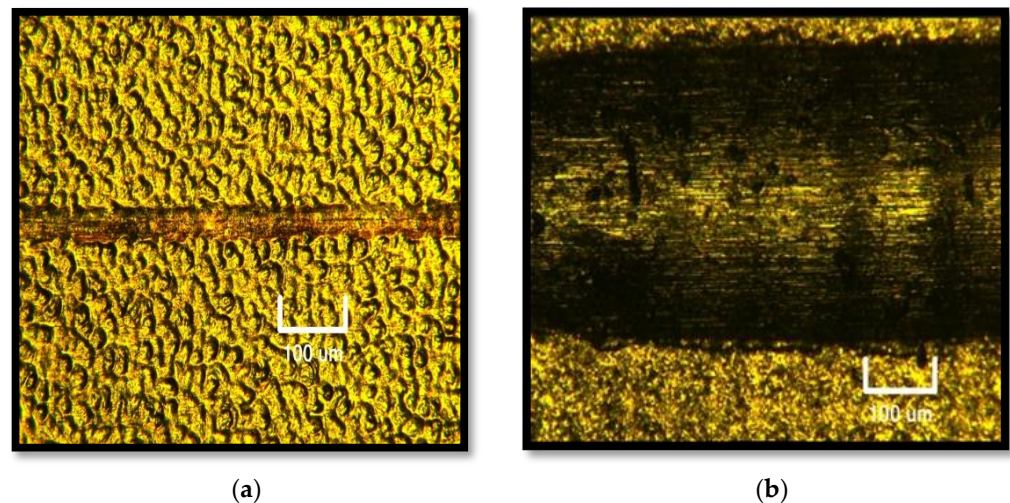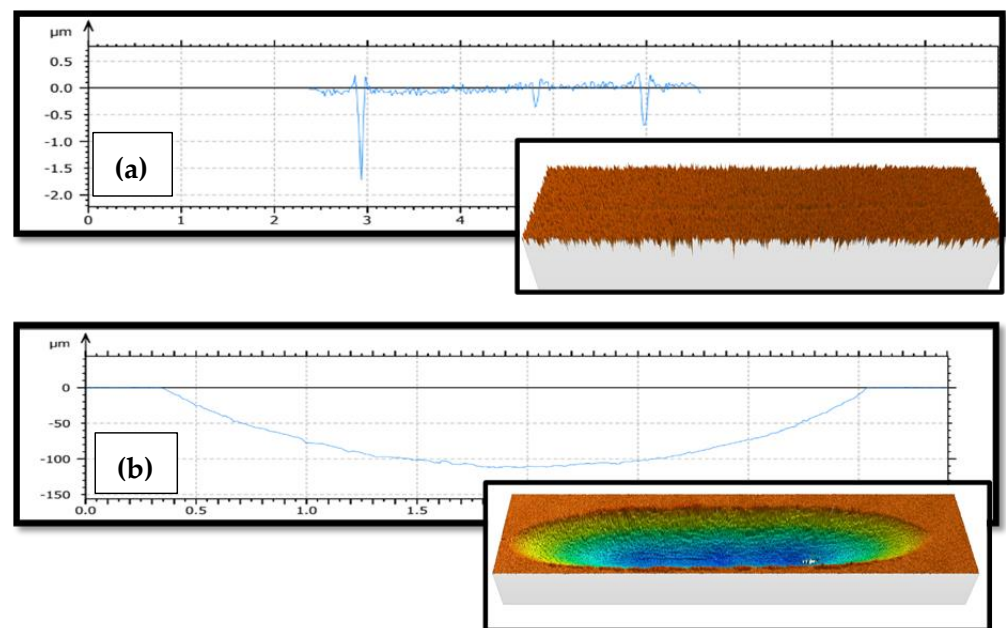

(**a**)　　　　　　　　　　　　　　　　　　　　　　　　　(**b**)

Figure 13. Optical images of worn surfaces: (**a**) sample with dimple density of 25 dimples/mm (sample 2) and (**b**) untextured sample.

Two- and three-dimensional profiles of sample 2 (25 dimples/mm) and the untextured surfaces are summarized in Figure 14. Again, negligible wear with only superficial scratching was observed on the textured surfaces. Under the same experimental conditions, a deeper and wider wear track was obtained with the untreated titanium surface.

Figure 14. Two- and three-dimensional wear track profiles of (**a**) sample with dimple density of 25 dimples/mm (sample 2) and (**b**) untextured sample.

Figure 15 shows the SEM images of the wear tracks for the untextured sample and the textured sample with 25 dimples/mm dimple density (sample 2). In the untextured sample, a severe component of three-body abrasive wear was observed, where some of the wear particles responsible for the ploughing effect could still be seen in the image (Figure 15a,b). Plastically deformed material at the wear track edges was also observed on the untreated surface. On the other hand, for the sample with a dimple density of 25 dimples/mm, a very smooth and superficial wear track was observed, where no deformation of material or trapped hard particles could be seen.
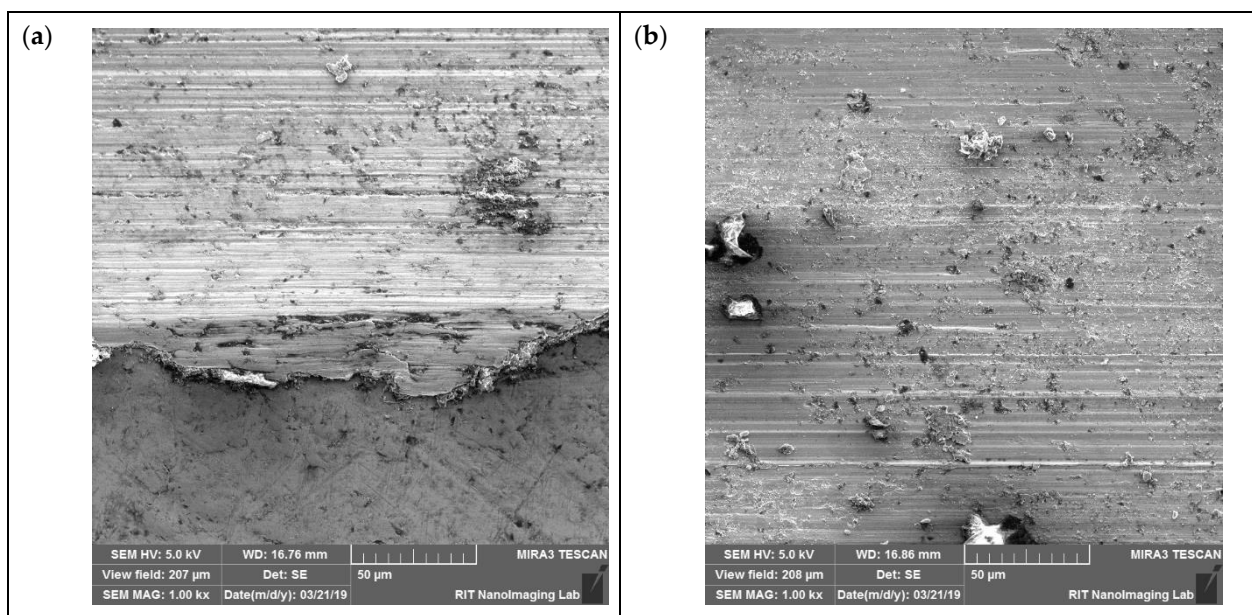
Figure 15. *Cont.*
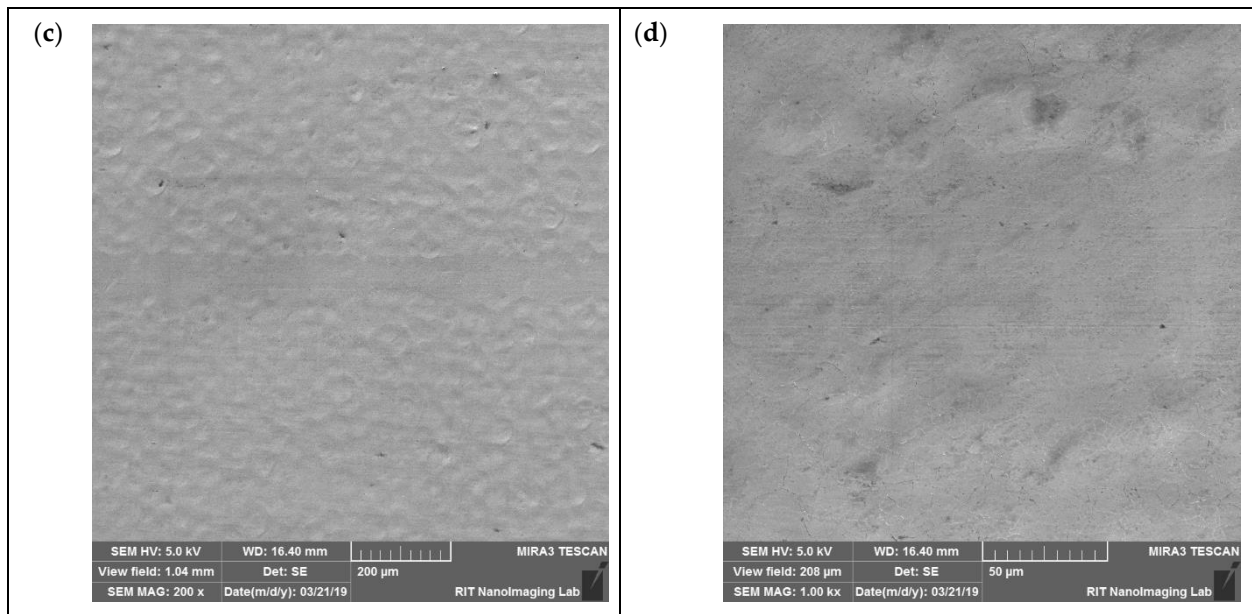
Figure 15. SEM images of wear tracks of (**a**,**b**) untextured sample, (**c**,**d**) sample with dimple density of 25 dimples/mm (sample 2).

4. Conclusions

In this work, the tribological properties of eight textured surfaces with different dimple densities, created by laser on titanium samples, were studied and compared to the results obtained on an untextured surface. Results showed that laser texturing helps to improve the tribological properties of the titanium alloy. For all of the textured surfaces, friction and wear were reduced as compared to the untextured sample. In particular:

- Samples with the highest dimple densities (sample 1 and sample 2), showed a friction reduction of around 67% and wear reduction of almost 99% with respect to the untextured surface.
- For the sample with the highest dimple density (50 dimples/mm), created with the lowest laser speed, an important increase in the surface hardness was observed due to longer exposure to laser treatment. This increased surface hardness may have influenced the tribological properties of the sample.
- Sample 2 with a dimple density of 25 dimples/mm showed a very low increase in surface hardness, with better tribological performance that could be attributed to the surface texturing effect.
- Samples with dimple densities ranging from 16.7 to 7.1 dimples/mm (sample 3 to sample 8) showed highly similar friction coefficients, which were slightly lower than that of the untextured sample, with an average reduction in friction of 6%. These samples presented low friction coefficients at the beginning of the test, when there were fresh dimples on their surfaces. However, as the test progressed, these dimples were worn out, and the effect of the textured surface was canceled. As a result, high friction values were observed through the rest of the test.
- The dimple wear-out time observed in samples 3 to 8 was greatly influenced by the dimple density.

References

1. Liu, Z.; He, B.; Lyu, T.; Zou, Y. A Review on Additive Manufacturing of Titanium Alloys for Aerospace Applications: Directed Energy Deposition and Beyond Ti-6Al-4V. *Jom* **2021**, *73*, 1804–1818. [CrossRef]
2. Zhao, Q.; Sun, Q.; Xin, S.; Chen, Y.; Wu, C.; Wang, H.; Xu, J.; Wan, M.; Zeng, W.; Zhao, Y. High-strength titanium alloys for aerospace engineering applications: A review on melting-forging process. *Mater. Sci. Eng. A* **2022**, *845*, 143260. [CrossRef]
3. Cecchel, S.; Montesano, L.; Cornacchia, G. Wear and Corrosion Characterization of a Ti–6Al–4V Component for Automotive Applications: Forging versus Selective Laser Melting Technologies. *Adv. Eng. Mater.* **2022**, *2200082*, 1–10. [CrossRef]
4. You, S.H.; Lee, J.H.; Oh, S.H. A Study on Cutting Characteristics in Turning Operations of Titanium Alloy used in Automobile. *Int. J. Precis. Eng. Manuf.* **2019**, *20*, 209–216. [CrossRef]
5. Aufa, A.N.; Hassan, M.Z.; Ismail, Z. Recent advances in Ti-6Al-4V additively manufactured by selective laser melting for biomedical implants: Prospect development. *J. Alloys Compd.* **2022**, *896*, 163072. [CrossRef]
6. Chirico, C.; Vaz Romero, A.; Gordo, E.; Tsipas, S.A. Improvement of wear resistance of low-cost powder metallurgy β-titanium alloys for biomedical applications. *Surf. Coat. Technol.* **2022**, *434*, 128207. [CrossRef]
7. Holmberg, K.; Erdemir, A. Influence of tribology on global energy consumption, costs and emissions. *Friction* **2017**, *5*, 263–284. [CrossRef]
8. Holmberg, K.; Erdemir, A. Tribology International The impact of tribology on energy use and CO_2 emission globally and in combustion engine and electric cars. *Tribol. Int.* **2019**, *135*, 389–396. [CrossRef]
9. Holmberg, K.; Andersson, P.; Erdemir, A. Global energy consumption due to friction in passenger cars. *Tribol. Int.* **2012**, *47*, 221–234. [CrossRef]
10. Solomon, S.; Plattner, G.-K.; Knutti, R.; Friedlingstein, P. Irreversible climate change due to carbon dioxide emissions. *Proc. Natl. Acad. Sci. USA* **2009**, *106*, 1704–1709. [CrossRef]
11. Holmberg, K.; Kivikytö-Reponen, P.; Härkisaari, P.; Valtonen, K.; Erdemir, A. Global energy consumption due to friction and wear in the mining industry. *Tribol. Int.* **2017**, *115*, 116–139. [CrossRef]
12. Bruzzone, A.A.G.; Costa, H.L.; Lonardo, P.M.; Lucca, D.A. Advances in engineered surfaces for functional performance. *CIRP Ann.-Manuf. Technol.* **2008**, *57*, 750–769. [CrossRef]
13. Iglesias, P.; Bermúdez, M.D.; Carrión, F.J.; Martínez-Nicolás, G.; Martínez-Nicolás, G. Friction and wear of aluminium-steel contacts lubricated with ordered fluids-neutral and ionic liquid crystals as oil additives. *Wear* **2004**, *256*, 386–392. [CrossRef]
14. Guo, H.; Smith, T.W.T.W.; Iglesias, P. The study of hexanoate-based protic ionic liquids used as lubricants in steel-steel contact. *J. Mol. Liq.* **2020**, *299*, 112208. [CrossRef]
15. Iglesias, P.; Bermúdez, M.D.; Moscoso, W.; Rao, B.C.; Shankar, M.R.; Chandrasekar, S. Friction and wear of nanostructured metals created by large strain extrusion machining. *Wear* **2007**, *263*, 636–642. [CrossRef]
16. Tock, A.; Saldana, C.; Iglesias, P. Tribological Performance of Textured Surfaces Created by Modulation-Assisted Machining. *J. Tribol.* **2018**, *140*, 061704. [CrossRef]
17. Mao, B.; Siddaiah, A.; Liao, Y.; Menezes, P.L. Laser surface texturing and related techniques for enhancing tribological performance of engineering materials: A review. *J. Manuf. Process.* **2020**, *53*, 153–173. [CrossRef]
18. Sasaki, S. Environmentally friendly tribology (Eco-tribology). *J. Mech. Sci. Technol.* **2010**, *24*, 67–71. [CrossRef]
19. Cao, W.; Hu, T.; Fan, H.; Hu, L. Laser surface texturing and tribological behaviour under solid lubrication on titanium and titanium alloy surfaces. *Int. J. Surf. Sci. Eng.* **2021**, *15*, 50–66. [CrossRef]
20. Daskalova, A.; Lasgorceix, M.; Bliznakova, I.; Angelova, L.; Hoquet, S.; Leriche, A.; Trifonov, A.; Buchvarov, I. Ultra-fast laser surface texturing of β-tricalcium phosphate (β-TCP) ceramics for bone-tissue engineering applications. In *Journal of Physics: Conference Series*; IOP Publishing: Bristol, UK, 2020; Volume 1492. [CrossRef]
21. De La Guerra Ochoa, E.; Otero, J.E.; Tanarro, E.C.; Morgado, P.L.; Lantada, A.D.; Munoz-Guijosa, J.M.; Sanz, J.M. Optimising lubricated friction coefficient by surface texturing. *Proc. Inst. Mech. Eng. Part C J. Mech. Eng. Sci.* **2013**, *227*, 2610–2619. [CrossRef]
22. Tang, W.; Zhou, Y.; Zhu, H.; Yang, H. The effect of surface texturing on reducing the friction and wear of steel under lubricated sliding contact. *Appl. Surf. Sci.* **2013**, *273*, 199–204. [CrossRef]
23. Yuan, S.; Huang, W.; Wang, X. Orientation effects of micro-grooves on sliding surfaces. *Tribol. Int.* **2011**, *44*, 1047–1054. [CrossRef]
24. Gualtieri, E.; Borghi, A.; Calabri, L.; Pugno, N.; Valeri, S. Increasing nanohardness and reducing friction of nitride steel by laser surface texturing $. *Tribol. Int.* **2009**, *42*, 699–705. [CrossRef]
25. Zhang, H.; Hua, M.; Dong, G.N.; Zhang, D.Y.; Chin, K.S. A mixed lubrication model for studying tribological behaviors of surface texturing. *Tribol. Int.* **2016**, *93*, 583–592. [CrossRef]
26. Ronen, A.; Etsion, I.; Kligerman, Y. Friction-reducing surface-texturing in reciprocating automotive components. *Tribol. Trans.* **2001**, *44*, 359–366. [CrossRef]
27. Etsion, I.; Sher, E. Improving fuel efficiency with laser surface textured piston rings. *Tribol. Int.* **2009**, *42*, 542–547. [CrossRef]

28. Khaskhoussi, A.; Risitano, G.; Calabrese, L.; D'andrea, D. Investigation of the Wettability Properties of Different Textured Lead/Lead-Free Bronze Coatings. *Lubricants* **2022**, *10*, 82. [CrossRef]

29. Volpe, A.; Covella, S.; Gaudiuso, C.; Ancona, A. Improving the laser texture strategy to get superhydrophobic aluminum alloy surfaces. *Coatings* **2021**, *11*, 369. [CrossRef]

30. Pang, M.; Liu, X.; Liu, K. Effect of wettability on the friction of a laser-textured cemented carbide surface in dilute cutting fluid. *Adv. Mech. Eng.* **2017**, *9*, 1687814017738154. [CrossRef]

31. Akbarzadeh, S.; Khonsari, M.M. Effect of surface pattern on stribeck curve. *Tribol. Lett.* **2010**, *37*, 477–486. [CrossRef]

32. Wang, X.; Liu, W.; Zhou, F.; Zhu, D. Preliminary investigation of the effect of dimple size on friction in line contacts. *Tribol. Int.* **2009**, *42*, 1118–1123. [CrossRef]

33. Salguero, J.; Del Sol, I.; Vazquez-Martinez, J.M.; Schertzer, M.J.; Iglesias, P. Effect of laser parameters on the tribological behavior of Ti6Al4V titanium microtextures under lubricated conditions. *Wear* **2019**, *426–427*, 1272–1279. [CrossRef]

34. Senatore, A.; Risitano, G.; Scappaticci, L.; D'andrea, D. Investigation of the tribological properties of different textured lead bronze coatings under severe load conditions. *Lubricants* **2021**, *9*, 34. [CrossRef]

35. Abril, S.O.; Del Socorro Fonseca-Vigoya, M.; Pabón-León, J. CFD Analysis of the Effect of Dimples and Cylinder Liner Honing Groove on the Tribological Characteristics of a Low Displacement Engine. *Lubricants* **2022**, *10*, 61. [CrossRef]

36. Niu, Y.; Pang, X.; Yue, S.; Shangguan, B.; Zhang, Y. The friction and wear behavior of laser textured surfaces in non-conformal contact under starved lubrication. *Wear* **2021**, *476*, 203723. [CrossRef]

37. Ullah, M.Z.; Rizwan, M.; Raza, A.; Ahmed, A.; Abid, M. Effect of dimple shape and depth on tribological performance of textured surface. In Proceedings of the 2021 18th International Bhurban Conference on Applied Sciences and Technologies, Islamabad, Pakistan, 12–16 January 2021; pp. 719–725. [CrossRef]

38. Kligerman, Y.; Etsion, I.; Shinkarenko, A. Improving Tribological Performance of Piston Rings by Partial Surface Texturing. *J. Tribol.* **2005**, *127*, 632. [CrossRef]

39. Mehta, P.; Liu, R.; Mann, J.B.; Saldana, C.; Iglesias, P. Effect of textured surfaces created by modulation-assisted machining on the Stribeck curve and wear properties of steel-aluminum contact. *Int. J. Adv. Manuf. Technol.* **2018**, *99*, 399–409. [CrossRef]

40. Byun, J.W.; Shin, H.S.; Kwon, M.H.; Kim, B.H.; Chu, C.N. Surface texturing by micro ECM for friction reduction. *Int. J. Precis. Eng. Manuf.* **2010**, *11*, 747–753. [CrossRef]

41. Costa, H.; Hutchings, I. Some innovative surface texturing techniques for tribological purposes. *Proc. Inst. Mech. Eng. Part J J. Eng. Tribol.* **2015**, *229*, 429–448. [CrossRef]

42. Scaraggi, M.; Mezzapesa, F.P.; Carbone, G.; Ancona, A.; Sorgente, D.; Lugarà, P.M. Minimize friction of lubricated laser-microtextured-surfaces by tuning microholes depth. *Tribol. Int.* **2014**, *75*, 123–127. [CrossRef]

43. Qu, J.; Truhan, J.J. An efficient method for accurately determining wear volumes of sliders with non-flat wear scars and compound curvatures. *Wear* **2006**, *261*, 848–855. [CrossRef]

44. Schertzer, M.J.; Iglesias, P. Meta-Analysis Comparing Wettability Parameters and the Effect of Wettability on Friction Coefficient in Lubrication. *Lubricants* **2018**, *6*, 70. [CrossRef]

45. Bombard, A.J.F.; Gonçalves, F.R.; Shahrivar, K.; Ortiz, A.L.; de Vicente, J. Tribological behavior of ionic liquid-based magnetorheological fluids in steel and polymeric point contacts. *Tribol. Int.* **2015**, *81*, 309–320. [CrossRef]

46. Matczak, L.; Johanning, C.; Gil, E.; Smith, T.W.T.W.; Schertzer, M.J.M.; Iglesias Victoria, P.; Guo, H.; Smith, T.W.T.W.; Schertzer, M.J.M.; Iglesias, P. Effect of cation nature on the lubricating and physicochemical properties of three ionic liquids. *Tribol. Int.* **2018**, *124*, 23–33. [CrossRef]

47. Qu, J.; Truhan, J.J.; Dai, S.; Luo, H.; Blau, P.J. Ionic liquids with ammonium cations as lubricants or additives. *Tribol. Lett.* **2006**, *22*, 207–214. [CrossRef]

48. Vidyasagar, K.E.C.; Pandey, R.K.; Kalyanasundaram, D. An exploration of frictional and vibrational behaviors of textured deep groove ball bearing in the vicinity of requisite minimum load. *Friction* **2021**, *9*, 1749–1765. [CrossRef]

49. Syed, I.; Sarangi, M. Hydrodynamic lubrication with deterministic micro textures considering fluid inertia effect. *Tribol. Int.* **2014**, *69*, 30–38. [CrossRef]

50. Liu, W.; Ni, H.; Chen, H.; Wang, P. Numerical simulation and experimental investigation on tribological performance of micro-dimples textured surface under hydrodynamic lubrication. *Int. J. Mech. Sci.* **2019**, *163*, 105095. [CrossRef]

51. Xue, X.; Lu, L.; Wang, Z.; Li, Y.; Guan, Y. Improving tribological behavior of laser textured Ti-20Zr-10Nb-4Ta alloy with dimple surface. *Mater. Lett.* **2021**, *305*, 130876. [CrossRef]

52. Wang, Y.-Q.; Wu, G.-F.; Han, Q.-G.; Fang, L.; Ge, S.R. Tribological properties of surface dimple-textured by pellet-pressing. *Procedia Earth Planet. Sci.* **2009**, *1*, 1513–1518. [CrossRef]